Computer simulation study on the swelling of a model polymer network by a chainlike solvent

Z.-Y. Lu and R. Hentschke*
FB Physik, Bergische Universität-Gesamthochschule, D-42097 Wuppertal, Germany
(Received 1 October 2001; revised manuscript received 7 January 2002; published 12 April 2002)

A molecular-dynamics–particle-transfer method was used to study the swelling of a model polymer network by a short chain solvent. The solvent chains were transferred depending on the difference between the solvent chemical potentials in the coupled simulation boxes, containing pure solvent and gel, respectively. The chemical potentials were computed via the Rosenbluth sampling method. The simulated swelling ratio of the network under subcritical and supercritical conditions is compared with the prediction of a modified Flory-Huggins theory. In addition, the chains exhibit markedly different structural and dynamic properties in the corresponding phases due to the constraint imposed by the network, which are discussed in detail.

DOI: 10.1103/PhysRevE.65.041807 PACS number(s): 61.25.Hq, 05.10.−a, 05.50.+q, 05.20.−y

I. INTRODUCTION

The relation between the molecular structure of a polymer network and its swelling behavior due to the adsorption of solvent is difficult to establish on the microscopic level. This is because experimentally it is difficult to synthesize polymer networks with well defined structure. On the other hand it is easy to study a defect-free polymer network in computer simulations. And thus a significant number of simulation studies focusing on the structural and dynamic properties of polymer networks already exist [1–8]. Simulations of the swelling of gels, which explicitly include solvent molecules, are scarce, however. Recently, Kenkare *et al*. have used combined discontinuous molecular dynamics and Monte Carlo simulations to study the swelling of athermal polymer networks containing a hard-sphere solvent [9]. They also proposed an analytical theory as an extension of their previous work [10] and found that the theoretical results coincide with their simulations. In a grand canonical-type ensemble, Escobedo and de Pablo have used the Monte Carlo method to discuss the swelling of athermal [11], square well, and modified Lennard-Jones polymer networks [12]. They report on simulation results for the solvent fraction and the network packing fraction as a function of temperature and pressure. In addition, the effects of network chain length were also investigated. The simulation results are in good agreement with their equations of state [11] for the hard-sphere network and with a combined Sanchez-Lacombe–Flory-Rehner theory [12,13] for a soft-sphere network, respectively. Using a newly developed Gibbs-ensemble molecular dynamics method [14,15], Aydt and Hentschke reported dynamic as well as structural results for swelling equilibria in model network-solvent systems using Lennard-Jones nonbonded interactions [16].

The present work is a part of a systematic computer study of network swelling using explicit solvent, where a first paper, Ref. [17], dealt with one-center solvents and was used to develop the general algorithm. Note that in Ref. [17] we used the expression ''one site'' instead of ''one center.'' To avoid any misleading connection to lattice simulations we adopt ''center'' throughout this paper. In Ref. [17] a combined molecular-dynamics–Widom-test-particle method was used and the results were compared to an extended Flory-Huggins model. This allowed us to extend simulation data or fill gaps in the latter, and thus avoid computationally expensive simulations. The complex swelling behavior under subcritical as well as under supercritical conditions was attributed to the competing effects of the excess solvent chemical potential difference and the solvent density ratio computed for the two phases (i.e., the pure bulk solvent and the solvent in the gel). The present paper is intended to modify and extend the algorithm to allow for chainlike solvents, and to study their effects. It should be noted that not only the development of an algorithm including chainlike solvent is of interest, but the swelling of a network by a chainlike solvent and the solvent behavior inside the network are also of great practical interest in the petroleum industry. We use a similar method as in Ref. [17] to investigate the swelling of a model network by a subcritical as well as supercritical multicenter (six-center) solvent. During the molecular dynamics simulations the solvent chemical potentials are calculated via the Rosenbluth sampling method [18] instead of the Widom-test-particle method [19]. The resulting solvent chemical potentials in the network simulation cell and in a simulation cell containing bulk solvent only (at identical thermodynamic conditions) are used to transfer solvent particles between the simulation cells until chemical equilibrium is attained.

The proposed simulation method is generally useful and effective for studying chemical equilibria of polymer networks in contact with explicit solvent under variable thermodynamic conditions. For example, our algorithm, in contrast to pure Monte Carlo methods, also allows the study of diffusion of solvent inside the network as a function of temperature and pressure. In this work, we mainly discuss the temperature and pressure dependences of the network swelling ratio q. The modified Flory-Huggins theory described in Ref. [17], which previously was found to yield an excellent qualitative description of the system for a one-center solvent, is found to be less good in the present case. Furthermore, the dependence of the solvent conformation on the different thermodynamic conditions is also discussed. The self-diffusion of the solvent in the network and in the bulk phase are calculated via the Einstein relation. Their comparison illustrates

*Author to whom correspondence should be addressed.

 ©2002 The American Physical Society

the hindrance effects due to the network beads on the solvent diffusion. Finally, the chain end-to-end autocorrelation function is obtained showing different relaxation times in the network as compared to the bulk solvent.

II. SIMULATION METHOD AND MODEL CONSTRUCTION

In this paper, we continue to use the ''two-box–particle-transfer'' method introduced in Ref. [17]. Here two simulation boxes will reach chemical equilibrium by exchanging solvent particles. One of the boxes contains solvent only, whereas the other contains the model polymer network penetrated by solvent particles. The latter are chainlike particles consisting of six sequentially bonded interaction centers. The solvent exchange is controlled by direct comparison of the respective solvent chemical potentials that we calculate via Rosenbluth sampling. The simple cubic model network, used in all simulations, is the same as in Ref. [16], i.e., every second interaction center along a network chain is a cross link with sixfold coordination. The sixfold coordination is somewhat unusual, because it is not realized in real chemical networks. However, the cubic structure is a convenient simplification, which does not alter the qualitative effects.

The solvent chemical potential in the two boxes, $\mu_\alpha(\alpha=0,1)$, can be written as [20]

$$\mu_\alpha=\mu_\alpha^{id}+\mu_\alpha^{ex}, \tag{1}$$

where μ_α^{id}, the ideal gas chemical potential, is given by

$$\mu_\alpha^{id}=k_BT\ln\left[\frac{(N_\alpha+1)\Lambda^3}{\langle V_\alpha\rangle}\right]. \tag{2}$$

Here, $N_\alpha(\alpha=0,1)$ is the number of solvent particles in simulation box α with volume V_α, Λ is the thermal wavelength of the solvent, k_B is the Boltzmann constant, and T is the temperature. μ_α^{ex}, the excess part of the chemical potential, can be calculated via the Rosenbluth sampling method [20] via

$$\mu_\alpha^{ex}=-k_BT\ln\left[\frac{\langle V_\alpha W\rangle}{\langle V_\alpha\rangle}\right], \tag{3}$$

where W is the Rosenbluth factor. $\langle\rangle$ in the above equations denotes ensemble averages under constant temperature and pressure conditions. For a certain chain configuration n, the Rosenbluth factor reads

$$W(n)=\prod_{i=1}^{l}\frac{w_i}{k}, \tag{4}$$

where w_i is defined via

$$w_i=\sum_{j=1}^{k}\exp[-\beta u_i(j)]. \tag{5}$$

Here $l=5$ is the number of chain segments or bonds, k is the total number of segment orientations, and $\beta=1/k_BT$. The orientation of a segment is defined via the torsion angle ϕ between the plane spanned by the previous two segments and the plane spanned by the previous segment and the current segment. Here ϕ is an integral multiple of $2\pi/k$. Note that using a large value of k, i.e., $k=50$, improves the sampling. Equations (4) and (5) are implemented as follows. An already existing chain is extended by a bond i, whose direction in space j is chosen with probability $\{\exp[-\beta u_i(j)]\}/w_i$. Here $u_i(j)$ includes all interactions of the newly added segment with the rest of the chain as well as the interactions with all other chains. Because the k possible orientations of segment i depend on the segments $i-1$ and $i-2$, the first two chain segments are special. They are constructed as the extensions of a virtual chain consisting of two bonds, which is inserted in the system at a random point and with random orientation.

The potential energy $\mathcal{U}$ in each simulation box is given by $\mathcal{U}=\mathcal{U}_{LJ}+\mathcal{U}_{net}+\mathcal{U}_{val}$, where $\mathcal{U}_{LJ}$ is the nonbonded Lennard-Jones potential energy, $\mathcal{U}_{net}$, which equals zero in the solvent box, is the interaction energy between bonded network beads, and $\mathcal{U}_{val}$ is the intramolecular valence energy of the six-center solvent. The first two terms are introduced in the previous paper [17]; in addition, we have the intramolecular valence potential

$$\mathcal{U}_{val}=u_{bond}+u_{bend}+u_{tors}, \tag{6}$$

in which

$$u_{bond}=\sum_{\langle ij\rangle}\frac{k_{ij}^b}{2}(l_{ij}-l_{0,ij})^2, \tag{7}$$

$$u_{bend}=\sum_{\langle ijk\rangle}\frac{k_{ijk}^\theta}{2}(\theta_{ijk}-\theta_{0,ijk})^2, \tag{8}$$

and

$$u_{tors}=\sum_{\langle ijkl\rangle}c_1[1+\cos(\phi_{ijkl})]+c_2[1-\cos(2\phi_{ijkl})]+c_3[1+\cos(3\phi_{ijkl})]. \tag{9}$$

Here, k_{ij}^b is the bond stretching force constant, $l_{0,ij}$ is the equilibrium bond length, k_{ijk}^θ is the valence angle force constant, and $\theta_{0,ijk}$ is the equilibrium valence angle. The torsion energy is considered in Eq. (9), where c_1, c_2, and c_3 are parameters [21]. The notation $\langle ij\rangle$ means that the summation includes all the pairs of i and j, which are directly bonded. Similarly the notation $\langle ijk\rangle$ refers to all bond angles formed by the triples i, j, and k. And, finally, $\langle ijkl\rangle$ includes all quadruples belonging to all possible dihedral angles. All force field parameters together with the thermostat and the barostat coupling constants are compiled in Table I.

The equations of motion governing the time evolution in each individual simulation box are the same as in Ref. [17], i.e., we continue to use the weak coupling method due to Berendsen *et al.* [22]. The equations of motion are integrated via the leapfrog algorithm [23]. The solvent exchange between boxes, on the other hand, is governed by the following procedure. During the N-P-T simulation, the solvent chemi-

TABLE I. The force field parameters and the thermostat and barostat parameters. The six-center solvent is represented by C_3-$(C_2)_4$-C_3. N_N represents the network centers. Note that we have scaled the units to make $T_c^{solvent}=P_c^{solvent}=1$ in our system.

Lennard-Jones	σ	ϵ	m
C_2	0.2829	0.0902	1.0000
C_3	0.2980	0.1933	1.0713
N_N	0.3629	0.2924	1.1426
Bond stretch	k^b	l_0	
C_3-C_2	8708.27	0.1162	
C_2-C_2	8708.27	0.1162	
N_N-N_N	1674.67	0.4526	
Angle bend	k^θ[rad^{-2}]	θ_0[°]	
C_3-C_2-C_2	123.11	114.0	
C_2-C_2-C_2	123.11	114.0	
Torsion	c_1	c_2	c_3
X-C_2-C_2-X	0.6988	−0.1338	1.5582
Parameter	Value		
Δt	1.2073		
τ_T	120.73		
τ_P/κ_T	249.36		

cal potentials in the two simulation boxes are continuously calculated via the Rosenbluth sampling method as described above. The averages $\langle\rangle$ are thereby based on 1.2×10^4 trial chains constructed during 4×10^3 time steps at randomly selected locations in each box. Other numbers of trial chains and time intervals were also tested extensively. In particular, it was ensured that the result is independent on the procedure. The solvent exchange between the two simulation boxes is controlled by direct comparison of the so computed solvent chemical potentials. Each six-center solvent particle is associated with a transfer variable ξ, that has the value of 0 or 1 depending on whether the solvent particle resides in the network box or in the solvent box. This means that all terms in the expression for the total energy involving solvent particle i are multiplied by ξ_i in one box and by $1-\xi_i$ in the other. A solvent chain is transferred by changing its ξ value from 0 to 1 or from 1 to 0 attempting to reduce the chemical potential difference. This transfer is instantaneous, i.e., a randomly selected solvent chain in one box will be forced into the other box without any attempt to change its conformation during the transfer. For the chain length and densities considered here, this simple transfer method is fully sufficient.

Initially, we start the simulation with 256 nontransferable network beads and 24 solvent chains distributed homogeneously in box 0, whereas box 1 contains 192 solvent chains. To relax the unfavorable initial network geometry, a 10^5 time step N-V-T simulation is executed without solvent transfer. Subsequently, the N-P-T simulation is carried out allowing solvent exchange. Typical simulation runs range from 1×10^6 to 2×10^6 total time steps.

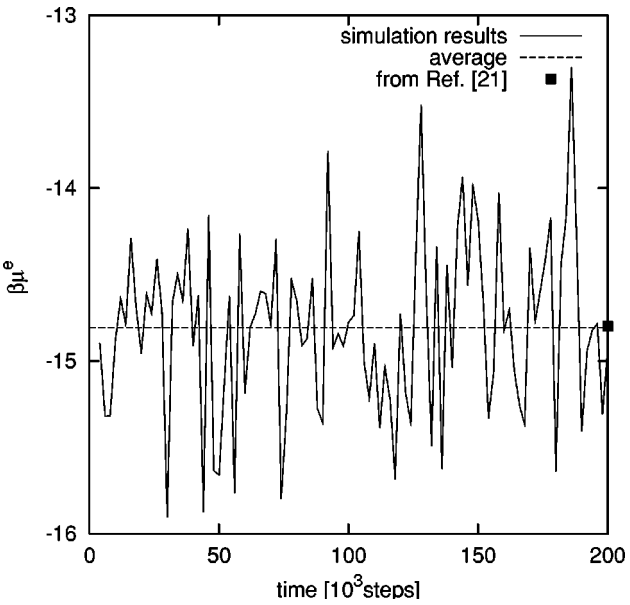

FIG. 1. Reduced excess chemical potential ($\beta\mu^e$) calculated via the Rosenbluth sampling method. Solid line: present work; dashed line: corresponding average; symbol: result taken from Ref. [24].

III. RESULTS AND DISCUSSION

To our knowledge, there are no reports on the chemical potential of our six-center solvent under the conditions considered here. However, Frenkel *et al.* have calculated the excess chemical potentials of continuously deformable chains [24] based on the Rosenbluth algorithm. By switching off the inner constraints of the six-center solvent molecule (putting u_{bend} and u_{tors} equal to zero), we obtain the continuously deformable chain just mentioned, and thus we may compare our results to the corresponding results in Ref. [24]. The result is shown in Fig. 1. The number of six-center chains is $N=216$, the number of trial insertions is $N_{ins}=4\times10^4$, and the number of possible orientations for one bond is $k=50$. Under the same conditions as in Ref. [24], i.e., $\rho^*=\rho\sigma^3=0.6$ and $T^*=k_BT/\epsilon=1.2$, where σ and ϵ are the Lennard-Jones parameters of one interaction center, we can reproduce the result of Frenkel *et al.* very accurately.

To make the discussion more transparent, we scale the simulation temperatures and pressures by the corresponding critical values of the bulk solvent, i.e., $T_r=T/T_c$ takes on the values 0.89, 1.05, 1.26, and 1.64, and $P_r=P/P_c$ takes on the values 1.30, 2.17, 3.29, 4.34, 6.52, 8.69, 10.86, and 13.02. In addition, we carry out extra simulations at $P_r=3.82$ and 4.05 for $T_r=0.89$, and at $P_r=2.43$ and 2.72 for $T_r=1.05$, respectively, showing the sharp change of the swelling ratio q close to the critical temperature of the pure solvent (see below).

For these values of T_r and P_r, Fig. 2(a) shows the resulting swelling ratios q. If we compare these q values to the corresponding result for the one-center solvent shown in Fig. 3 of Ref. [17], we notice that the overall magnitude of q is greatly reduced in the present case of the chainlike solvent. The $T_r=1.64$ curve shows a monotonous rise with increasing pressure (with an apparent maximum at high P_r). This behavior is qualitatively similar to the swelling behavior ob-

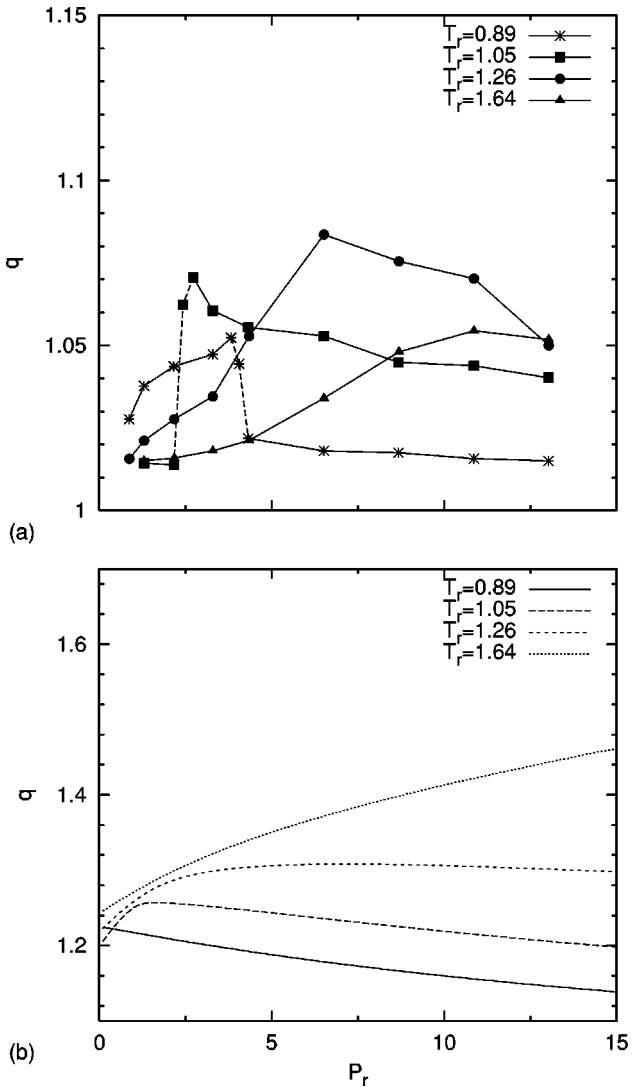

FIG. 2. The $q-P_r$ isotherms. The symbols in (a) are the simulation results. The lines in (b) represent the results of the modified Flory-Huggins theory [17]. Here $\chi=0.7/T_r-0.3$, $\chi_1=0.992/T_r$, and $\chi_2=0.3/T_r+1.1$.

tained for the one-center solvent at high T_r. The next curve, $T_r=1.26$, again exhibits an initial increase of q with increasing P_r. But this time there is a broad maximum and a subsequent decrease of q. Again this is qualitatively similar to the behavior of the one-center solvent as T_r approaches 1. For the one-center solvent at $T_r=1.05$ we obtained a steep increase of q at low P_r and a subsequent slow decrease. For the six-center solvent we likewise observe a steep increase and a subsequent slow decrease. For $T_r<1$, i.e., $T_r=0.89$, we obtain a slow increase of q with decreasing pressure, which ends with a sudden rise. This once more is analogous to our corresponding result for the one-center solvent. Except here, this behavior appears inverted compared to the $T_r=1.05$ curve.

Figure 2(b) shows the isotherms obtained from our modified Flory-Huggins model [17]. Comparing Figs. 2(b) and 2(a), we find that the modified Flory-Huggins lattice model does not quite yield the good qualitative agreement that we

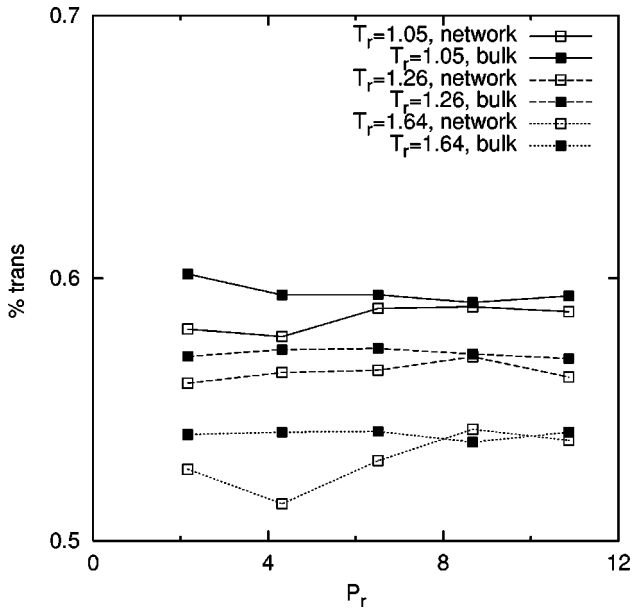

FIG. 3. The average percent *trans* torsion angles versus reduced pressure P_r.

found comparing theory and simulation in the case of the one-center solvent. The theory is explained in detail in Ref. [17]. It modifies the Flory-Huggins lattice model to include empty lattice centers, which makes the system compressible. This model contains three parameters, $\chi=-q_z(\epsilon_{11}+\epsilon_{22}-2\epsilon_{12})/2k_BT$, $\chi_1=-q_z\epsilon_{11}/2k_BT$, and $\chi_2=-q_z\epsilon_{22}/2k_BT$; q_z is the lattice coordination, and ϵ_{11}, ϵ_{22}, and ϵ_{12} are center-center interaction energies, where 1 indicates solvent and 2 indicates network centers). The interaction parameter χ_1 is obtained from the critical isotherm (cf. Ref. [17]). The other two parameters, χ and χ_2, are written as $\chi=uT_c/T+v$ and $\chi_2=u_2T_c/T+v_2$, where here u_2 and v_2 are slightly different from u_2 and v_2 used in Ref. [17]. The really new adjustable parameters are u and v that are adjusted to qualitatively fit the simulation result obtained at $T_r=0.89$ for large P_r. Notice that the theory also yields an increasing q at $T_r=1.64$, which is in accord with the simulation (except for large P_r, where the simulation result appears to decrease again). At $T_r=1.26$ we do find complete qualitative agreement between theory and simulation. At $T_r=1.05$ the theory yields a maximum at roughly the pressure where the simulated q exhibits an apparent jump. At the lowest temperature $T_r=0.89$, the theoretical q also decreases with increasing P_r, but again we do not obtain the jumplike feature produced by the simulation. There is, however, always the possibility that a combination of the parameters u, v, u_2, and v_2 is overlooked, which would yield an overall qualitative agreement.

Figure 3 compares the average percent *trans* states for the six-center solvent in the network and in the bulk solvent at different temperatures and pressures. The *trans* state is defined using the ''pseudocosine'' method [25]. This means that a torsion angle i is considered to be in the *trans* state, when the relationship $\xi_i(\phi_{max})\geqslant\overline{\xi_i}$ is satisfied, where

$$\overline{\xi_i} = \frac{\mathbf{b}_{i-1} \cdot \mathbf{b}_{i+1}}{b_{i-1} b_{i+1}}. \tag{10}$$

Here $\mathbf{b}_i$ is the bond vector between interaction centers i and $i+1$ of the six-center solvent, and $\xi_i(\phi_{max})$ is given by

$$\xi_i(\phi_{max}) = -\sin^2\theta_0 \cos\phi_{max} + \cos^2\theta_0, \tag{11}$$

where $\theta_0 = 114°$ is the equilibrium bond angle, and $\phi_{max} = 120°$ is the torsion barrier maximum. At lower pressures, the solvent molecules are more stretched in bulk state than in the network as reflected by the difference of the average percent *trans* shown in Fig. 3. With the increase of pressure, the overall difference decreases. This may be related to the density difference in the corresponding simulation boxes. At lower pressure, the network box represents a dense phase compared to the pure solvent box, and the network beads constrain the possible configurations of the solvent. We also find that as pressure increases, the percent *trans* states in the bulk solvent remains constant while the same quantity in network shows a slight overall increase. Increasing the temperature results in the well known reduction of *trans* states.

The dynamics of the solvent may be studied in part via its center of mass self-diffusion coefficient, which is calculated here via the Einstein relation [26],

$$D = \lim_{t\to\infty} \langle |\vec{r}_i(t) - \vec{r}_i(0)|^2 \rangle / 6t, \tag{12}$$

where $\vec{r}_i(t)$ is the position of molecule i at time t. In Fig. 4(a) $\ln D$ is plotted vs $1000/T$. Thus, assuming the Arrhenius behavior [27,28], we may calculate the activation energy from the slope of the fitted line. Figure 4(a) shows such a fit for the solvent in the network as well as in its bulk state at $P_r = 8.69$. Figure 4(b) shows the resulting ratios of the activation energies in network and in the bulk state versus pressure. Note that the activation energies of solvent self-diffusion in the network, E_N, are always smaller than the corresponding quantities in bulk, E_S. Moreover, with increasing pressure, the ratio E_N/E_S increases almost linearly. Notice, however, that $D_N < D_S$ also, as can be seen in Fig. 4(a) as well as in Fig. 5 discussed below. Since this implies that the ratio $D_N^{(0)}/D_S^{(0)} < 1$, using the notation $D = D^{(0)}\exp(-E/k_BT)$, we may infer that either the frequency of attempted molecular jumps or the number of suitable holes permitting a jump or both is significantly reduced in the network. There is no apparent reason for the first possibility, and thus the reduction of suitable holes appears most likely under the conditions used here. Figure 5 shows the ratio D_N/D_S vs P_r, where D_N is the self-diffusion coefficient of the solvent in the gel, and D_S is the corresponding quantity in the bulk solvent. At all temperatures the ratio increases gradually with increasing pressure, which indicates that the hindrance effects on the solvent diffusion due to the network decrease at higher pressures. The same is true for fixed P_r and decreasing T_r. Comparing with Fig. 7(c) of Ref. [17], we find that if the same network is swollen by a one-center solvent, the ratio D_N/D_S overall behaves similarly.

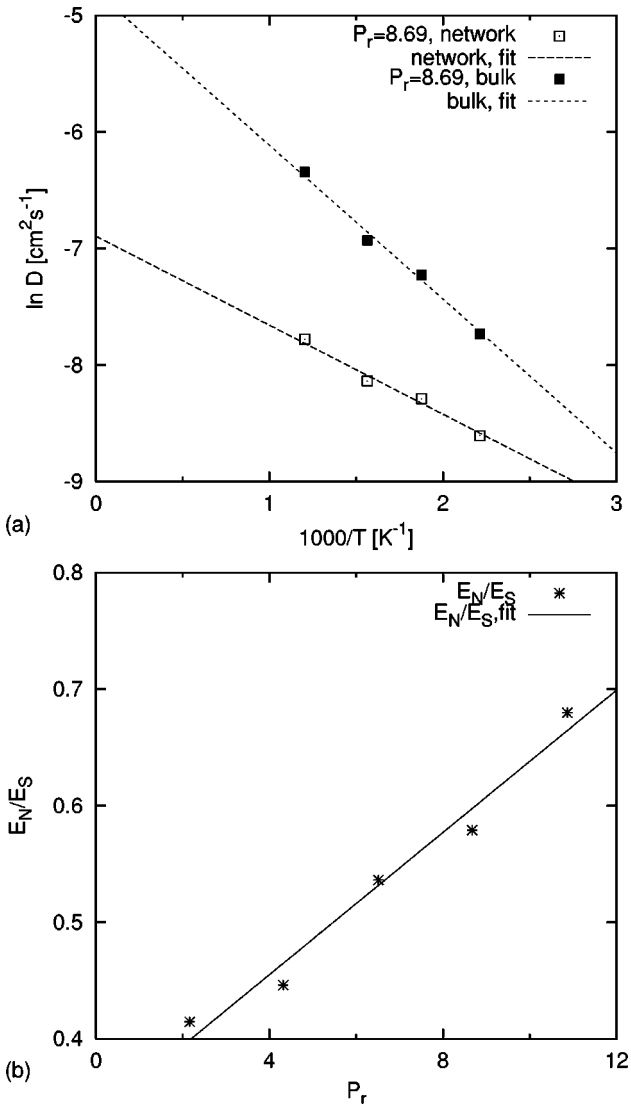

FIG. 4. (a) The $\ln D$ vs $1000/T$. The symbols represent simulation results and the lines are linear fits. (b) The resulting ratios of the solvent self-diffusion activation energies in the network and in the bulk, E_N/E_S, vs reduced pressure P_r.

Another interesting dynamic property is the chain reorientation relaxation. We define end-to-end vector autocorrelation functions for the solvent via

$$P_1(t) = \langle \mathbf{R}(t) \cdot \mathbf{R}(0) \rangle, \tag{13}$$

$$P_2(t) = \frac{1}{2}(3\langle [\mathbf{R}(t) \cdot \mathbf{R}(0)]^2 \rangle - 1), \tag{14}$$

cf. Ref. [27], where $\mathbf{R}(t)$ is the unit end-to-end vector at time t. In the following, $P_1(t)$ and $P_2(t)$ are fitted to the empirical Kohlraush-Williams-Watts (KWW) equation [29]

$$P_1^{KWW}(t) = \exp[-(t/\tau_1)^{\beta_1}], \tag{15}$$

$$P_2^{KWW}(t) = \exp[-(t/\tau_2)^{\beta_2}], \tag{16}$$

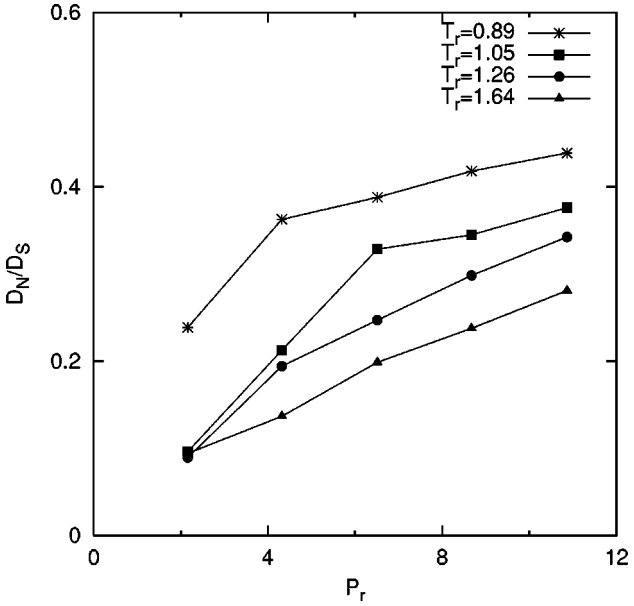

FIG. 5. The ratio of the solvent self-diffusion coefficients in the network and in the bulk, D_N/D_S, as a function of reduced pressure P_r. The symbols are the results of the simulations, whereas the lines serve to guide the eye.

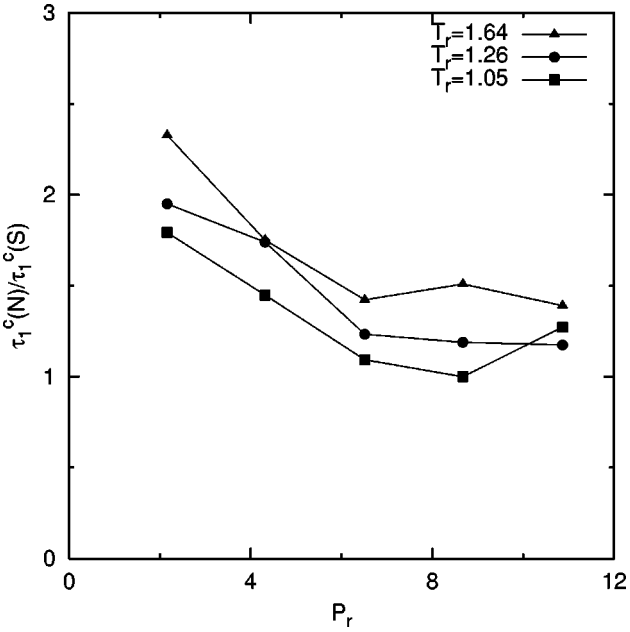

FIG. 7. $\tau_1^c(N)/\tau_1^c(S)$ as a function of reduced pressure P_r. The symbols are the simulation results, and the lines serve to guide the eye.

where τ_k and β_k $(k=1,2)$ are parameters. Assuming that $P_1(t)$ and $P_2(t)$ approach zero at long times, the characteristic time constants are $\tau_1^c=\int_0^\infty dt P_1(t)$ and $\tau_2^c=\int_0^\infty dt P_2(t)$, respectively [27,30]. Figure 6 shows $P_1(t)$ calculated via Eq. (13) and the corresponding fitted curve obtained via Eq. (15) for two typical simulation conditions. Large departures of β from 1 (we observe an overall variation ranging from 1.1 to 1.9) reflect the complexity of the end-to-end vector relaxation. As a function of P_r between 2.17 and 10.86, the ratio τ_1^c/τ_2^c ranges from 1.827 to 2.407 at $T_r=0.89$ and from 1.496 to 1.887 at $T_r=1.64$ in the bulk solvent. It ranges from 2.128 to 3.085 at $T_r=0.89$ and from 1.950 to 2.684 at $T_r=1.64$ in the network. In the network as well as in the bulk solvent, we find that the ratio decreases with increasing temperature. Furthermore, the values in the network are higher than the corresponding values in the bulk solvent. The τ_1^c/τ_2^c is directly related to the nature of rotation process, i.e., $\tau_1^c/\tau_2^c=3.0$ indicates an isotropic rotational diffusion and smaller values indicate large angular jumps of the molecules [31]. Therefore, here it is easier to activate large angular jumps with increasing temperature. Besides the ratio τ_1^c/τ_2^c, the network effects on the relaxation of the end-to-end vector are also of interest. In Fig. 7, the ratio of $\tau_1^c(N)/\tau_1^c(S)$ is plotted vs P_r, where $\tau_1^c(N)$ is the characteristic relaxation time in the network, and $\tau_1^c(S)$ is the corresponding quantity in the bulk solvent. Generally, the ratio tends to 1.0 with increasing pressure. This shows that the hindrance effect due to the network is larger at lower pressure, where the relaxation time in the network is close to twice that in the bulk solvent. Notice that when the pressure increases, the solvent box has a similar density as the network box, therefore, the hindrance effects from network beads are not as apparent as before. Notice also that $\tau_1^c(N)/\tau_1^c(S)$ increases with increasing temperature.

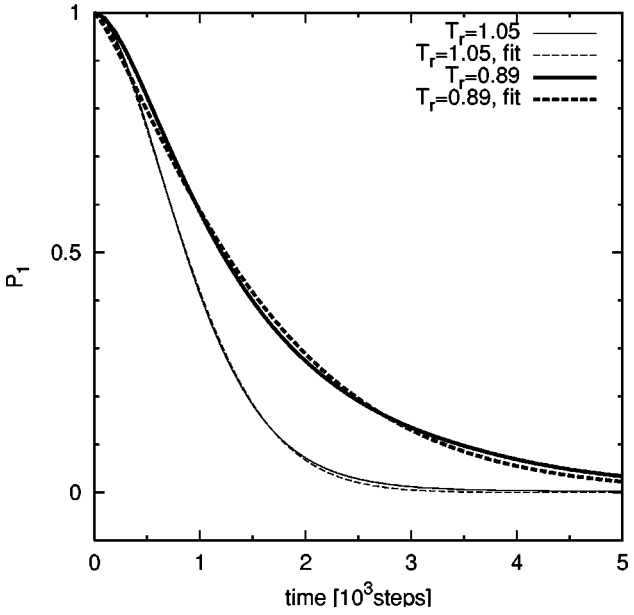

FIG. 6. P_1 as a function of time. The solid lines are the simulation results and the dashed lines are fitted curves calculated via Eq. (15). For $T_r=1.05$, $P_r=4.34$, $\beta_1=1.6318$, and $\tau_1=1.0878$; for $T_r=0.89$, $P_r=4.34$, $\beta_1=1.2201$, and $\tau_1=1.6732$.

IV. CONCLUSION

The present work is a part of a systematic computer study of network swelling using an explicit solvent. In Ref. [17] and in this work, where we focus on a short-chain solvent, we have developed an algorithm, that can be used to study not only swelling of a polymer network by an explicit sol-

vent, but more generally the chemical equilibrium of a polymer network in contact with an explicit solvent under variable thermodynamic conditions. For example, our algorithm, in contrast to pure Monte Carlo methods, also allows the study of diffusion of solvent inside the network as a function of temperature and pressure (and with some known modifications also under anisotropic external stress). This is an important aspect in industrial studies of the performance of adhesives (e.g., environmental attack on adhesive joints [32]).

Also in Ref. [17] we have obtained a simple analytic theory with the motivation to extend or fill gaps in the data obtained via the computationally expensive simulations. The most suitable candidate was seemed to be the simple Flory-Huggins mean field model. Even though this is a very simple lattice model, it can be shown to yield a good description of the thermodynamics of many real systems (such as alkane mixtures; this has been shown for instance in Ref. [33]). Our extension contains parameters, as does the original model, which can be adjusted to the simulation data in order to allow the above mentioned predictions beyond or in between simulation results. This idea works nicely for small solvents [17] and for networks with increased mesh size. It may not be much good, however, for larger solvents as we show here, i.e., here the model could use improvement. Currently, work is in progress in which we systematically vary the mesh size of the model network as well as the solvent size [34].

[1] *Monte Carlo and Molecular Dynamics Simulations in Polymer Science*, edited by K. Binder (Oxford University Press, Oxford, 1995), Chap. 4, p. 194.

[2] Y.-K. Leung and B.E. Eichinger, J. Chem. Phys. **80**, 3877 (1984).

[3] K.-J. Lee and B.E. Eichinger, Polymer **31**, 406 (1990).

[4] J. Gao and J.H. Weiner, Macromolecules **20**, 2525 (1987).

[5] J. Gao and J.H. Weiner, Macromolecules **27**, 1201 (1994).

[6] E.R. Duering, K. Kremer, and G.S. Grest, J. Chem. Phys. **101**, 8169 (1994).

[7] J.U. Sommer, T.A. Vilgis, and G. Heinrich, J. Chem. Phys. **100**, 9181 (1994).

[8] R. Everaers and K. Kremer, Phys. Rev. E **53**, R37 (1996).

[9] N.R. Kenkare, C.K. Hall, and S.A. Khan, J. Chem. Phys. **113**, 404 (2000).

[10] N.R. Kenkare, C.K. Hall, and S.A. Khan, J. Chem. Phys. **110**, 7556 (1999).

[11] F.A. Escobedo and J.J. de Pablo, J. Chem. Phys. **106**, 793 (1997).

[12] F.A. Escobedo and J.J. de Pablo, J. Chem. Phys. **110**, 1290 (1999).

[13] M. Marchetti, S. Prager, and E.L. Cussler, Macromolecules **23**, 1760 (1990).

[14] M.J. Kotelyanskii and R. Hentschke, Phys. Rev. E **51**, 5116 (1995).

[15] M.J. Kotelyanskii and R. Hentschke, Mol. Simul. **17**, 95 (1996).

[16] E.M. Aydt and R. Hentschke, J. Chem. Phys. **112**, 5480 (2000).

[17] Z.-Y. Lu and R. Hentschke, Phys. Rev. E **63**, 051801 (2001).

[18] M.N. Rosenbluth and A.W. Rosenbluth, J. Chem. Phys. **23**, 356 (1955).

[19] B. Widom, J. Chem. Phys. **39**, 2802 (1963).

[20] D. Frenkel and B. Smit, *Understanding Molecular Simulation: From Algorithms to Applications* (Academic Press, San Diego, 1996).

[21] M.G. Martin and J.I. Siepmann, J. Phys. Chem. B **102**, 2569 (1998).

[22] H.J.C. Berendsen, J.P.M. Postma, W.F. van Gunsteren, A. DiNola, and J.R. Haak, J. Chem. Phys. **81**, 3684 (1984).

[23] R.W. Hockney, Methods Comput. Phys. **9**, 136 (1970).

[24] D. Frenkel, G.C.A.M. Mooij, and B. Smit, J. Phys.: Condens. Matter **3**, 3053 (1991).

[25] T.A. Weber, J. Chem. Phys. **69**, 2347 (1978).

[26] M. P. Allen and D. J. Tildesley, *Computer Simulations of Liquids* (Oxford Science, Oxford, 1987).

[27] G.D. Smith and D.Y. Yoon, J. Chem. Phys. **100**, 649 (1994).

[28] N.F.A. van der Vegt, Macromolecules **33**, 3153 (2000).

[29] G. Williams and D.C. Watts, Trans. Faraday Soc. **66**, 80 (1970).

[30] R.C. Runnebaum and E.J. Maginn, J. Phys. Chem. B **101**, 6394 (1997).

[31] G.F. Signorini, J.-L. Barrat, and M.L. Klein, J. Chem. Phys. **92**, 1294 (1990).

[32] P. Frantzis, JSME Int. J., Ser. A **41**, 231 (1998).

[33] R. Koningsveld and L.A. Kleintjens, Acta Polym. **39**, 341 (1988).

[34] Z.-Y. Lu and R. Hentschke (unpublished).